Article

J. Mex. Chem. Soc. **2025**, *69*(3)
Regular Issue
©2025, Sociedad Química de México
ISSN-e 2594-0317

Metformin Adsorption on Binuclear Boron Schiff Complexes

Marisol Ibarra-Rodríguez[1], Víctor M. Jiménez-Pérez[1], Blanca M. Muñoz-Flores[1], Mario Sánchez[2]

[1]Universidad Autónoma de Nuevo León, Facultad de Ciencias Químicas, Ciudad Universitaria, San Nicolás de los Garza, 66455, Nuevo León, México.
[2]Centro de Investigación en Materiales Avanzados, S.C., Alianza Norte 202, PIIT, Carretera Monterrey-Aeropuerto Km. 10, C. P. 66628, Apodaca, Nuevo León, México.

***Corresponding author:** Marisol Ibarra-Rodríguez, email: mibarod_22@hotmail.com; Víctor M. Jiménez-Pérez, email: victor.jimenezpr@uanl.edu.mx; Mario Sánchez, email: mario.sanchez@cimav.edu.mx

Received January 22nd, 2024; Accepted October 2nd, 2024.

DOI: http://dx.doi.org/10.29356/jmcs.v69i3.2207

Abstract. Metformin (*N, N*-dimethylbiguanidine) is a drug with many biological functions. In certain cases, it is necessary for this compound to interact with some molecules in order to increase the efficacy of administration in the human body. For this purpose, density functional theory was used to study the intermolecular interactions between binuclear boron Schiff complexes and metformin (charged and neutral). All structures herein, have been studied by using Natural and Mulliken charges, Natural Bond Orbitals (NBO), and quantum molecular descriptors. The adsorption energies (E_{ads}) for the most stable structures with neutral metformin are -27.02 to -53.34 kcal/mol in gas phase. The E_{ads} for two monoprotonated metformin shows -39.71 kcal/mol in gas phase and -84.08 kcal/mol in water. The NBO results showed that the donor orbitals belong to the nitrogen atoms of metformin, while the acceptor orbitals belong to the C-H atoms of tert-butyl groups in binuclear boron Schiff complexes. The binuclear structure could be used as an adsorber and as a carrier of metformin molecules.
Keywords: Binuclear boron Schiff complexes; metformin; adsorption; DFT.

Resumen. La metformina(*N,N*-dimetilbiguanidina) es un fármaco con múltiples funciones biológicas. En ciertos casos, es necesario que este compuesto interactúe con ciertas moléculas para aumentar la eficacia de su administración en el cuerpo humano. Para ello, se empleó la teoría del funcional de la densidad para estudiar las interacciones intermoleculares entre los complejos de Schiff de boro binucleares y la metformina (con carga y neutra). Todas las estructuras aquí descritas se han estudiado utilizando cargas naturales y de Mulliken, orbitales de enlace naturales (NBO) y descriptores moleculares cuánticos. Las energías de adsorción (Eads) para la mayoría de las estructuras estables con metformina neutra son de -27.2 a -53.34 kcal/mol en fase gaseosa. Las Eads para dos metforminas monoprotonadas muestran -39.71 kcal/mol en fase gaseosa y -84.08 kcal/mol en agua. Los resultados del NBO mostraron que los orbitales donantes pertenecen a los átomos de nitrógeno de la metformina, mientras que los orbitales aceptores pertenecen a los átomos C-H de los grupos ter-butilos en los complejos de Schiff de boro binucleares. La estructura binuclear podría utilizarse como adsorbente y transportador de moléculas de metformina.
Palabras clave: Complejos de boro Schiff binucleares; metformina; adsorción; DFT.

Introduction

Diabetes mellitus is a disease that many people suffer nowadays. One drug to alleviate this metabolic disorder is metformin,[1] such is the case that the demand for metformin is increasing day by day.[2-5] Additionally, Studies have shown that metformin is associated with lower cancer mortality in type 2 diabetes.[6]

J. Mex. Chem. Soc. **2025**, *69*(3)
Regular Issue
©2025, Sociedad Química de México
ISSN-e 2594-0317

After oral ingestion of metformin, an incomplete absorption of about 40 to 60 % has been reported, this is due to degradation in the intestinal tract. [7-10] For this reason, the design and understanding of the electronic and structural behavior of new drug carriers that allow the controlled release of metformin in full doses offers a great opportunity for the proposal of new structures, which could be more efficient in the adsorption process.[11] Murthy Kolapalli et al. studied a metformin-HCl drug delivery system, using polymers, observing the advantage to retain the dosage form in the effective absorption site for long period of time.[12] Another research group studied the C_{60}, C_{48}, SiC_{59}, SiC_{47}, GeC_{59}, and GeC_{47} nanoclusters, which showed that metformin-nanocluster interactions are exothermic with high adsorption values.[13] Moreover, Rebitski *et al*. used two layered clays, a natural Wyoming montmorillonite, to encapsulate metformin. They found that Laponite allows a complete release of the charged drug.[14] Similarly, Mirzaei *et al.* studied the chitosan as a possible vehicle for carrying metformin.[15]

On the other hand, the doped boron nitride fullerenes are other materials were investigated to evaluate the adsorption capacity of the metformin molecule. This theoretical study was performed using the B3LYP-D and PW91-D functionals. Mahon reported that metformin exhibits chemical adsorption on $B_{12}N_{12}$ and $B_{16}N_{16}$.[16] Table 1 shows the theoretical adsorption studies of metformin.

An improvement in drug release is by implementing new molecules capable of adapting to aqueous media. Chemical and physical properties such as solubility, stability, and bioavailability can be modified using structures with different functional groups. [17,18] Recently, we have reported the synthesis and characterization of a series of boron Schiff bases as fluorescent dyes of silk fibroin and *in vitro* cell staining. [19,20] These molecules can be structurally modified to improve their properties. The crystal structure showed interactions with acetone molecules.[21]

In the present work, we have studied the adsorption of metformin molecule on binuclear boron Shiff complexes (BBSC). Our hypothesis is that BBSC and metformin will form strong interactions and with the help of the DFT and the Natural Bond Orbital theory (NBO) we will evaluate the values of the energies and nature of those interactions. [17,18]

Table 1. Adsorption of metformin molecule in different molecular systems.

System	Adsorption energies (kcal/mol)	Method	Ref.
Pristine Si, Al doped (single-wall carbon nanotubes)	-32.70 to -48.70	B3LYP/6-311G(d,p)	[22]
C_{60}, C_{48}, SiC_{59}, SiC_{47}, GeC_{59}, GeC_{47}	-22.70 to -54.41	B3PW91/6-311G(d,p)	[13]
Wyoming montmorillonite	-42.73	QEq (Charge equilibration method) and PBE	[14]
Chitosan	-10.10	B3LYP/6-311++G(d,p)	[15]
Doped boron nitride fullerenes	-37.20 to -78.20	B3LYP-D/PW91-D	[16]
Al-B nitride nanocones	-19.85	B3LYP/6-31G(d)	[23]
Chitosan-hydrogel		PM6	[24]
Cyclic peptides	-46.53	B3LYP/6-31++G (d,p)	[25]
Metal-Decorated $Mg_{12}O_{12}$ Nanoclusters	-50.4 to -94.6	B3LYP/6-311G(d,p)	[26]

Computational details

Binuclear boron Schiff complexe (**BBSC**), binuclear boron Schiff complex-Metformin (**A**) and binuclear boron Schiff complex-two metformin molecules (**B**) structures were optimized using the Perdew-

J. Mex. Chem. Soc. **2025**, *69*(3)
Regular Issue
©2025, Sociedad Química de México
ISSN-e 2594-0317

Burke-Ernzerhof (PBE0-D3) [27] functional and the 6-31G(d,p) basis set, with the Gaussian 09 program.[28] A DFT-D3 dispersion correction was performed with the Grimme's vdW correction in our calculations.[29] In order to characterize all optimized structures, we have computed their vibrational modes at the same level of theory. Geometries from local minima were used to carry out their respective NBO analysis, at the same level of theory.[30] The band gap for all systems were calculated from the difference between HOMO and LUMO orbitals. Adsorption energy E_{ads} were calculated through a single-point using the PBE0-D3 functional and the def2-TZVP basis set. [31,32] The adsorption energy, E_{ads}, is defined as the difference between the sum of the energy of the isolated molecule metformin and the BBSC-metformin. Adsorption energies (E_{ads}) of different systems were calculated with the following equation:

$$E_{ads}\,(\text{metformin}) = E\,(\text{BBSC-metformin}) - ((E\ \text{BBSC}) + (E\ \text{metformin}))$$

where E (BBSC-metformin) is the total energy of the system, and E BBSC and E metformin are the energies of the BBSC and metformin molecule, respectively.

The quantum molecular descriptors for BBSC and BBSC-metformin consist of ionization potential (I), electron affinity (A), global hardness (η), [33] electronegativity (χ), electronic chemical potential (μ), [34] electrophilicity index (ω) [35] and chemical softness (S) are calculated according to follows equations:

$$I = -E_{\mathrm{HOMO}},\ A = -E_{\mathrm{LUMO}},\ \eta = (I - A)/2,\ \chi = I + A/2,\ \mu = -(I + A)/2,\ \omega = -\mu^2/2\eta,\ \text{and}\ S = 1/2\eta$$

All generated files from Gaussian 09 were analyzed with the Chemcraft program v1.8

Results and discussion

The adsorption of metformin molecules on BBSC

We have optimized the binuclear boron Schiff complexes, whose experimental data have already been reported. [21] In addition, our results agree very well with the metformin geometry, previously reported, using the PBE0-D3/6-31G(d,p) method.[36]

As an initial step, in attempt to know the reactive zones where the metformin molecules could interact, the molecular electrostatic potential map (MESP) for the BBSC was calculated. The resulting MESP maps are characterized by consisting of various colors ranging from red to dark blue indicating the extreme negative and positive sites. It can also be related to the electronegativity of atoms. High electronegativity is observed with red color, while low electronegativity with blue color. Scheme 1 shows the active sites high in electron density located on the oxygen atoms. The sites low in electron density are located on the imine carbons with the imine protons. Additionally, the electron density of the aromatic rings and the low proton density of the tert-butyl groups are shown. The metformin molecule distributes into spaces (holes) to coordinate with electron-deficient sites.

Scheme 1 shows how two metformin molecules, through their nitrogen or hydrogen atoms, can interact with the **BBSC** molecule.

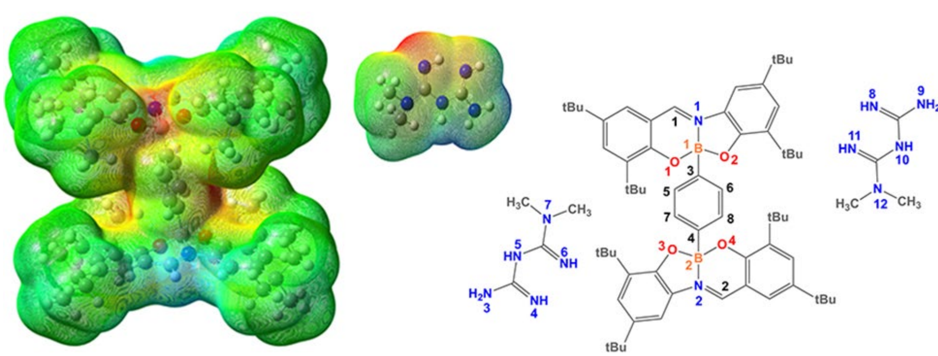

Scheme 1. Molecular electrostatic potential map for the **BBSC**, metformin and its possible interaction sites for the adsorption of metformins.

J. Mex. Chem. Soc. **2025**, *69*(3)
Regular Issue
©2025, Sociedad Química de México
ISSN-e 2594-0317

As a next step, the global minimum of the interaction of **BBSC** with a single (**A**) and two (**B**) metformin molecules was studied (Fig. 1). Based on our results shown in Table 2, B-O, B-N, B-C bond lengths and B-O-N angles values, for the **BBSC** fragment, were similar for both complexes (**A** and **B**), which are in accordance with previous experimental and computational results.[21,36]

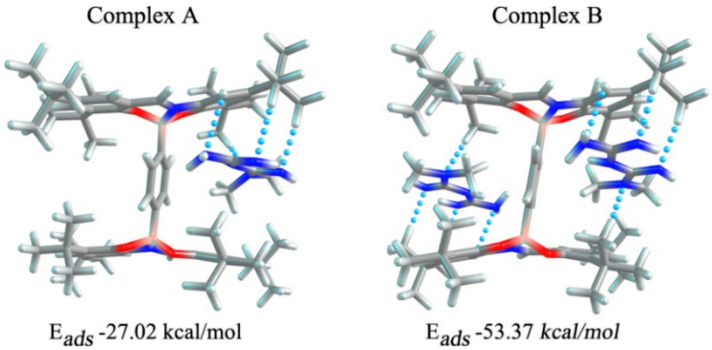

Fig. 1. Structural geometries for **complexes A** and **B**. Color code: dark gray (C); blue (N); white (H); pink (B); and red (O).

Table 2. Bond length (Å) and angle (°) values for the **BBSC** fragment in **A** and **B** complexes, computed with the PBE0-D3/6-31G(d,p) method.

	BBSC X-ray	**BBSC**	**Complex A**	**Complex B**
B1-O1	1.472	1.467	1.479	1.474
B1- O2	1.484	1.481	1.463	1.463
B1-N1	1.576	1.579	1.579	1.569
B1-C3	1.605	1.602	1.611	1.613
C3-C6	1.401	1.499	1.399	1.399
C6-C8	1.392	1.391	1.396	1.393
C8-C4	1.402	1.401	1.396	1.402
C4-C7	1.392	1.399	1.403	1.399
C4-B2	1.605	1.601	1.603	1.613
B2-O3	1.484	1.481	1.464	1.463
B2-O4	1.478	1.467	1.480	1.474
B2-N2	1.576	1.578	1.576	1.569
O2-B1-N1	106.5	106.50	106.85	106.96
O1-B1-N1	100.4	100.60	100.56	101.40
O4-B2-N2	106.5	106.51	107.17	106.96
O3-B2-N2	100.4	100.57	100.62	101.40

J. Mex. Chem. Soc. **2025**, *69*(3)
Regular Issue
©2025, Sociedad Química de México
ISSN-e 2594-0317

There are several weak interactions that together cause metformin molecules to be strongly attracted to the **BBSC**. For **complex A**, the adsorption is mainly through the N6 and H-C atoms of tert-butyl groups, forming hydrogen bonds with a distance value of 2.421 Å,[37] while for **complex B**, those hydrogen bonds are formed with the N6 and H-C (2.410 Å), N11 and H-C (2.412 Å) atoms of tert-butyl groups. Other weak interactions that help stabilize both complexes are: N_8---H-C, N_{11}---H-C, N_{12}---H-C. We can clearly observe that **BBSC** have short interatomic distances with the metformin (see Table 3).[38,39] The adsorption energy values in both complexes are very high, attributable to the hydrogen bonds (Fig. 1). These values are similar with the Si-walled carbon nanotubes and Al-walled carbon nanotubes systems, using the B3LYP functional.[22]

Natural charges on boron atoms are +1.103 to +1.105, after adsorption of metformin molecule for **complexes A** and **B**, respectively. These values are very similar for those shown on boron atoms in the **BBSC** structure before metformin coordination (+1.104).

Table 3. Selected H-bonds [Å] from calculated structures [D-H (D: donor) distance, H---A (A: acceptor) distance and D-H---A angle] of (**A, B)** using the PBE0-D3/6-31G(d,p) method.

	D-H	**H—A**	**D-H---A**
Complex A			
C-H---N_6	2.421	1.095	162.24
C-H---N4	2.665	1.095	166.84
C(6)---H-N_3	2.417	1.014	147.27
Complex B			
C-H---N8	2.500	1.095	165.54
C-H---N11	2.409	1.094	160.93
N9---H-Aromatic	3.030	1.080	105.65
C-H---N12	2.550	1.092	164.57
C-H---N4	2.412	1.094	160.85
C-H---N6	2.500	1.095	165.37
N3---H-Aromatic	3.030	1.083	106.70
C-H---N7	2.551	1.096	133.06

Frontier molecular orbital analysis and global reactivity parameters

The knowledge of frontier orbital energies is important for studying the chemical stability of compounds. [40] Energies for highest occupied molecular orbital (HOMO), lowest unoccupied molecular orbital (LUMO) and energy gaps (*Eg*), for both complexes, were calculated and presented in Table 4. The energy gaps show a slight increase after the adsorption of two metformins (0.03 eV), compared to the value of the free **BBSC**. Fig. 2, illustrates the HOMO and LUMO orbitals for **complex B**. In both complexes, the HOMO and LUMO are localized mainly on the aromatic groups of the ligand. The results indicate high stability of the complexes formed between metformin and **BBSC**.

On the other hand, the dipole moment values for **complexes A** and **B** are 6.49 and 0 Debyes, respectively. After adsorption one metformin molecule, the polarization increases (see Table 4), suggests an increased solubility of the resulting complex in a polar solvent. However, when two metformin molecules are adsorbed, there is a Ci symmetry because the metformin molecules are placed in opposite positions.

J. Mex. Chem. Soc. **2025**, *69*(3)
Regular Issue
©2025, Sociedad Química de México
ISSN-e 2594-0317

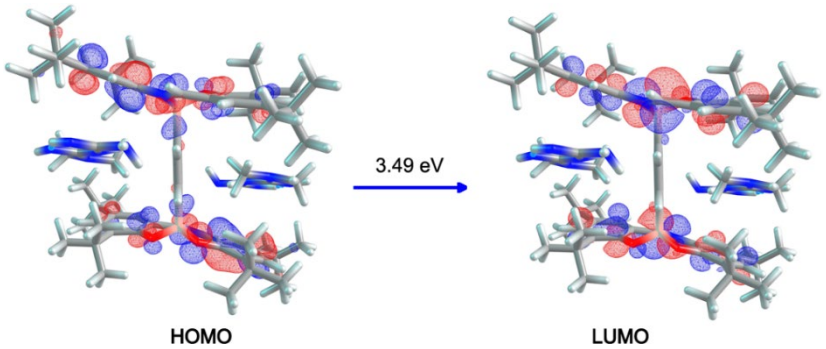

Fig. 2. HOMO and LUMO orbitals for **complex B**, calculated with the PBE0-D3/6-31G(d,p). Color code: dark gray (C), blue (N), white (H), pink (B), and red (O).

Also, the chemical potential (μ), global hardness (η), and electrophilicity index (ω), were calculated to for **BBSC**, **complex A** and **Complex B** structures. These chemical descriptors (μ), (η), and (ω) are shown in Table 4. Quantum molecular descriptors such as global hardness and electrophilicity index could be used to describe chemical reactivity and stability.[35] When one metformin are adsorbed on the **BBSC** structure, the value of η decrease slightly from 1.73 eV to 1.65 eV. These results indicate that the interaction of metformin molecule with boron Schiff base does not generate bond dissociation, indicating that the coordination is stable. The electrophilicity index (ω) value for **complex A and B** is slightly higher than for those values of **BBSC**. The higher values in **complexes A** and **B** mean that there is a better electrophilicity index, indicating that the **BBSC** structure acts as an electrophile, while the metformin molecule acts as a donor during the coordination.

In addition, the UV–Vis absorption spectra of the three structures were also studied. In order to know how much the UV-Vis absorption is affected when one or two metformin molecules are coordinated with the **BBSC**, the UV-Vis spectra were calculated. The absorption maximum band of **BBSC** (451 nm in gas phase) is similar to the experimental one (450 nm in methanol).[21] Coordination of one molecule of metformin on the **BBSC** structure shows a band at 452 nm. When the **BBSC** is coordinated to two metformin molecules, the spectrum shows an absorption band at 445 nm, attributed to π-π transitions.

In comparison, the UV-vis absorption values for **complex B** in different solvents were also calculated, using the polarizable continuum model (PCM). The results obtained are shown in Fig. 3**(b)**. The effect of the aqueous solvent causes a 8 nm decrease in absorption wavelengths. The presence of metformin molecules generates a slight hypochromic shift.

Table 4. Energies of frontier molecular orbitals (E_{HOMO}, E_{LUMO}, eV), HOMO-LUMO energy gaps (Eg, eV), calculated dipole moment (DM, Debye), global hardness (η, eV), chemical potential (μ, eV), and global electrophilicity index (ω, eV) for **BBSC** structure and for **complexes A** and **B** in gas phase.

	BBSC structure	**Complex A**	**Complex B**
λabs (nm)	451	452	445
E_{Homo} (eV)	-5.47	-5.72	-5.72
E_{Lumo} (eV)	-2.00	-2.23	-2.23
Band gap (eV)	3.46	3.31	3.49
D_M (debye)	0.0	6.49	0
I	5.47	5.72	5.72

J. Mex. Chem. Soc. **2025**, *69*(3)
Regular Issue
©2025, Sociedad Química de México
ISSN-e 2594-0317

	BBSC structure	**Complex A**	**Complex B**
A	2.00	2.23	2.23
χ	6.47	6.63	6.83
η (eV)	1.73	1.65	1.74
μ (eV)	-3.74	-3.87	-3.98
ω (eV)	4.03	4.52	4.53
S	0.289	0.30	0.29

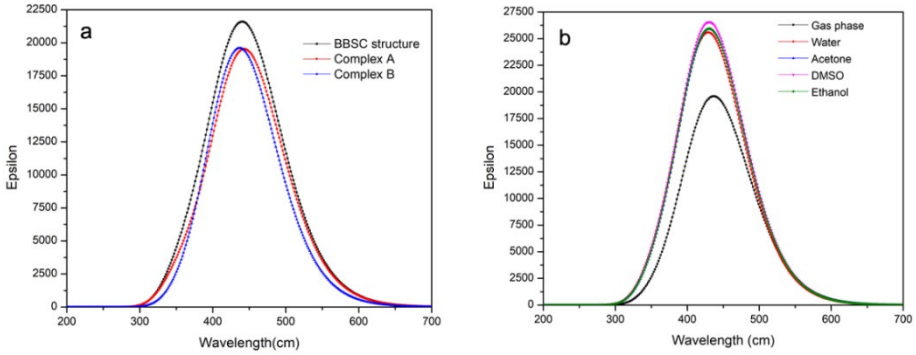

Fig. 3. **(a)** Theoretical UV-vis absorption spectra of **BBSC** structure and **complexes A** and **B**; **(b)** Theoretical UV-vis absorption spectra in different solvents for **complex B**.

One of the challenges is to know the physicochemical properties of metformin in aqueous solution. To, the adsorption energy of the systems studied in the aqueous phase was calculated. From the results it is observed that in the aqueous phase the adsorption of the metformin molecule on **BBSC** is lower than in the gas phase. See table 5. These data reveal that the drug release in the aqueous solution is easier than in gas phase. The **BBSC** has been used as a marker for carcinoma epidermoide A-431. The cytotoxicity studies reported by Jimenez and collaborators show high percentages of viability. These properties of boron complexes show advantages to be used as potent materials for the design of drug delivery. [21]

Table 5. Adsorption energies (E_{ads}) in gas phase and in water for **complexes A** and **B**.

Systems	E_{ads} **gas (kcal/mol)**	E_{ads} **in water (kcal/mol)**
Complex A	-27.02	-19.16
Complex B	-53.37	-36.86

NBO analysis

In order to characterize the charge transfer from one structure to another, we have performed an NBO analysis. [41] The evaluation of results shows that for all the configurations in gas phase are observed the $LP_{N6}\rightarrow\sigma^*_{C1\text{-}H}$, $LP_{N6}\rightarrow\sigma^*_{C1\text{-}H}$ and $LP_{N6}\rightarrow\sigma^*_{C1\text{-}H}$ interactions with energy values of 1.56, 1.76 and 1.75 kcal/mol,

J. Mex. Chem. Soc. **2025**, *69*(3)
Regular Issue
©2025, Sociedad Química de México
ISSN-e 2594-0317

respectively. As shown in the Table 6, Stabilization energy values show evidence of an interaction between N6 and N11 of metformin and C-H of *tert*-butyl groups. See Fig. 4.

Table 6. Donor and acceptor orbitals for the interactions from metformin molecules to **BBSC** structure**.**

Configuration	**Donor**	**Acceptor**	***E(2)* (kcal/mol)[a]**	***E(j)*-*E(i)* (a.u.)[b]**	**F(*i, j*) (a.u.)[c]**
Complex A	LP_{N6}	σ^*_{C-H}	1.56	0.88	0.034
Complex B	LP_{N6}	σ^*_{C-H}	1.76	0.87	0.036
	LP_{N11}	σ^*_{C-H}	1.75	0.88	0.036

[a]*E(2),* means energy of hyper conjugative interaction (stabilization energy)
[b]Energy difference between donor and acceptor *i* and *j* NBO orbitals
[c]*F*(*i*, *j*). is the Fock matrix element between *i* and *j* NBO orbitals

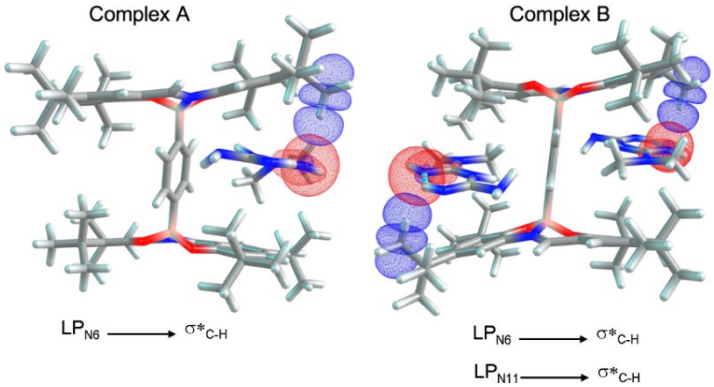

Fig. 4. Donor and acceptor orbitals responsible for intermolecular interactions. Color code: dark gray (C), blue (N), white (H), pink (B), and red (O).

Adsorption of protonated metformin on boron Schiff base

In a recently published study on the protonation of a metformin molecule, researchers found that at a pH of 4-11 it is mainly monoprotonated.[42,43]

Two monoprotonated metformin molecules were coordinated with the **BBSC** structure. The lowest energy structures are shown in Fig. 5**(a)**. The protonated metformin molecules were adsorbed in the central cavities formed by the *tert*-butyl groups of the **BBSC** structure.

We have found three main interactions, which are illustrated in Fig. 5**(a)**. These interactions are formed by the protons of the nitrogen of metformin with the carbon atoms of **BBSC**, the interactions are immediately placed: N10-H---C8-H (2.523 Å), N9-H---C3-H (2.398 Å), N11-H---C (2.544 Å), N3-H---C4-H (2.398 Å), N5-H---C5-H (2.526 Å) and N6-H-- -C (2.544 Å).

The band gap (*Eg*) value for the **biprotonated complex**, is 3.45 eV. Also, the adsorption energy was computed in gas phase (-84.08 kcal/mol) and simulating an aqueous solution (-39.71 kcal/mol).

The effect of the water solvent causes a decrease in the adsorption energy to -44.37 kcal/mol. The wavelength maximum absorption values of the **biprotonated complex** in gas is 451 nm, the water solvent decrease the 11 nm in the absorption.

J. Mex. Chem. Soc. **2025**, *69*(3)
Regular Issue
©2025, Sociedad Química de México
ISSN-e 2594-0317

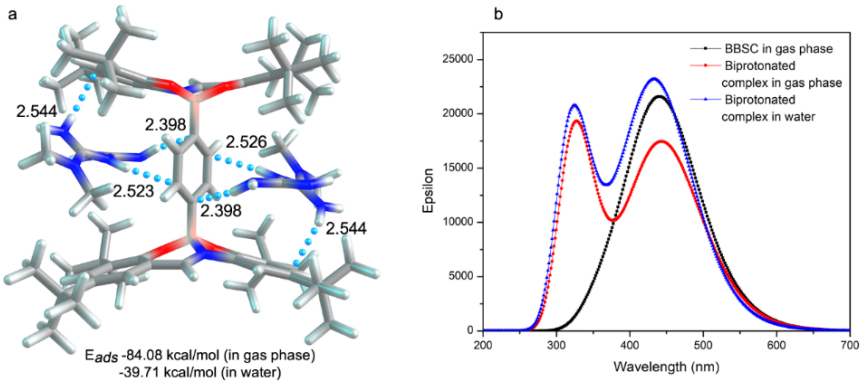

Fig. 5. **(a)** Side view of the **biprotonated complex**, with two metformin molecules interacting with imine hydrogens. Color code: dark gray (C); blue (N); white (H); pink (B); and red (O). **(b)** Theoretical UV-vis absorption spectra of **BBSC** structure and **Biprotonated complexes** in gas phase and water.

Finally, Fig. 6 shows the MESP of **complex B** and the **biprotonated complex**. The difference in positive regions (blue) and negative regions (red) is evident. The **biprotonated** structure shows more positive regions around the metformin molecules, which in **complex B** showed red areas, due to the extra protons included.

The MESP results predict a better interaction between the biprotoned complex and aqueous phase, the protonated metformin molecules show positive regions which can be solvated with water molecules. The above described is not observed in complex B.

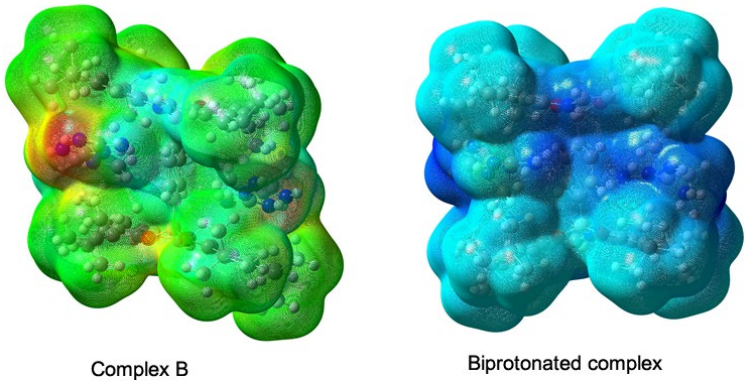

Fig. 6. Molecular electrostatic potential map for **complex B** and the **biprotonated complex**.

Table 7 shows the quantum molecular descriptors in the solvated. Solvation in **complexes A** and **B** causes a slight increase in global hardness, chemical potential, electrophilicity index and band gap. In the **biprotonated** system, solvation generates a decrease in chemical potential attributed to the decrease in polarizability. The stability of the **biprotonated complex** is predicted with the negative value of chemical potential (-4.27 eV). The **biprotonated complex** shows a decrease in the electrophilicity index when it is solvated, indicating that it is a bad electrophile.

J. Mex. Chem. Soc. **2025**, *69*(3)
Regular Issue
©2025, Sociedad Química de México
ISSN-e 2594-0317

Table 7. Energies of frontier molecular orbitals (E_{HOMO}, E_{LUMO}, eV), HOMO-LUMO energy gaps (*Eg*, eV), calculated dipole moment (DM, Debye), global hardness (η, eV), chemical potential (μ, eV), and global electrophilicity index (ω, eV) for **BBSC** structure and for **complexes A**, **B** and **Biprotonated** in water.

	BBSC structure	**Complex A**	**Complex B**	**Biprotonated**
E_{ads} (Kcal/mol)		-19.16	-36.86	-39.71
E_{Homo} (eV)	-5.757	-5.774	-5.779	-6.054
E_{Lumo} (eV)	-2.182	-2.203	-2.194	-2.497
Band gap (eV)	3.58	3.57	3.59	3.56
D_M (debye)	0	7.48	0.01	0
I	5.757	5.774	5.779	6.054
A	2.182	2.203	2.194	2.497
χ	6.848	6.876	6.876	7.303
η (eV)	1.788	1.786	1.793	1.779
μ (eV)	-3.969	-3.988	-3.987	-4.275
ω (eV)	4.407	4.454	4.433	5.139
S	0.278	0.279	0.279	0.281

Conclusions

Binuclear boron structure with a Schiff base and metformin molecules were studied with the help of density functional theory. Our results suggest that interacting metformin molecules can interact with the binuclear boron Schiff complex at high energy values. The negative complexation energies refer to the stability of the adsorption process. NBO analysis was used to characterize the intermolecular interactions and evidenced charge transfer from the nitrogen atoms of the metformin molecule to the C-H of tert-butyl groups of the **BBSC**. In addition, the evidence of such interaction is also supported by the electronics properties, such as, adsorption energy and quantum molecular descriptors.

In contrast, the adsorption of two protonated molecules of metformin with the **BBSC** shows a higher energy adsorption compared to metformin in neutral form. The effect of the water solvent causes a decrease in the adsorption energy values. Theoretical results show that the **BBSC** complex has properties to be used as an adsorber of metformin drug.

Acknowledgments

Mario Sánchez: Supervision, Project administration, Funding acquisition, Writing - review & editing. Marisol Ibarra Rodriguez: Conceptualization, Methodology, Writing - original draft, Formal analysis, Validation. Víctor Jiménez Pérez: Supervision y conceptualization, Blanca Muñoz Flores: Conceptualization

J. Mex. Chem. Soc. **2025**, *69*(3)
Regular Issue
©2025, Sociedad Química de México
ISSN-e 2594-0317

References

1. Dunn, C. J.; Peters, D. H. *Drugs*. **1995**, *49*, 721-749.
2. Wang, Y. W.; He, S. J.; Feng, X.; Cheng, J.; Luo, Y. T.; Tian, L.; Huang, Q. *Drug Des. Dev. Ther.* **2017**, *11*, 2421-2429.
3. Shurrab, N. T.; Arafa, E. S. A. *Obes. Med.* **2020**, *17*, 100186.
4. Samuel, V. P.; Dahiya, R.; Singh, Y.; Gupta, G.; Sah, S. K.; Gubbiyappa, S. K.; Chellappan, D. K.; Dua, K. *J. Environ. Pathol. Toxicol. Oncol.* **2019**, *38*, 133-141.
5. Yu, H.; Zhong, X.; Gao, P.; Shi, J.; Wu, Z.; Guo, Z.; Wang, Z.; Song, Y. *Front. Endocrinol. (Lausanne)* **2019**, *10*, 617.
6. Landman, G. W.; Kleefstra, N.; Hateren, K. J. van; Groenier, K. H.; Gans, R. O.; Bilo, H. J. *Diabetes care.* **2010**, *33*, 322-326.
7. Song, R. *Diabetes care*. **2016**, *39*, 187-189.
8. Kim, A.; Mujumdar, S. K.; Siegel, R. A. *Chemosensors*. **2014**, *2*, 1-12.
9. Raju, D. B.; Sreenivas, R.; Varma, M. M. *J. Chem. Pharm. Res.* **2010**, *2*, 274-278
10. Graham, G. G.; Punt, J.; Arora, M.; Day, R. O.; Doogue, M. P.; Duong, J.; Furlong, T. J.; Greenfield, J. R.; Greenup, L. C.; Kirkpatrick, C. M.; Ray, J. E.; Timmins, P.; Williams, K. M. *Clin. Pharmacokinet.* **2011**, *50*, 81-98.
11. Chen, Y.; Shan, X.; Luo, C.; He, Z. *J. Pharm. Investig.* **2020**, *50*, 219-230.
12. Meka, V. S.; Gorajana, A.; Dharmanlingam, S. R.; Kolapalli, V. R. *Invest. Clin.* **2013**, *54*, 347-459.
13. Kamali, F.; Rajaei, G. E.; Mohajeri, S.; Shamel, A.; Khodadadi-Moghaddam, M. *Monatsh. Chem.* **2020**, *151*, 711-720.
14. Rebitski, E. P.; Darder, M.; Sainz-Diaz, C. I.; Carraro, R.; Aranda, P.; Ruiz-Hitzky, E. *Appl. Clay. Sci.* **2020**, *186*, 105418.
15. Mirzaei, M.; Gulseren, O.; Jafari, E.; Aramideh, M. *Iran. Chem. Commun.* **2019**, *1*, 334-343.
16. Ghasemi, A. S.; Taghartapeh, M. R.; Soltani, A.; Mahon, P. J. *J. Mol. Liq*. **2019**, *275*, 955-967.
17. Haddish-Berhane, N.; Rickus, J. L.; Haghighi, K. *Int. J. Nanomedicine.* **2007**, *2*, 315- 331.
18. Rangel, V. N.; Delgadillo, A. N.; Salas, A. C. *J. Nanomed. Res.* **2015**, *2*, 23.
19. Molina-Paredes, A. A.; Jiménez-Pérez, V. M.; Lara-Cerón, J. A.; Moggio, I.; Arias, E.; Santillán, R.; Sánchez, M.; Saucedo-Yañez, A.; Muñoz-Flores, B. M. *Appl. Organometal. Chem.* **2019**, *33*, e4609;
20. Ibarra-Rodríguez, M.; Muñoz-Flores, B. M.; Gómez-Treviño, A.; Chan-Navarro, R.; Berrones-Reyes, R. J.; Chávez-Reyes, A.; Dias, H. V. R.; Sánchez Vázquez, M.; Jiménez-Pérez, V. M. *Appl. Organometal. Chem.* **2019**, *33*, e4718.
21. Ibarra-Rodríguez, M.; Muñoz-Flores, B. M.; Dias, H.V. R.; Sánchez, M.; Gomez- Treviño, A.; Santillan, R.; Farfán, N.; Jiménez-Pérez, V. M. *J. Org. Chem.* **2017**, *82*, 2375-2385.
22. Hoseininezhad-Namin, M. S.; Pargolghasemi, P.; Alimohammadi, S.; Rad, A. S.; Taqavi, L. *Physica E Low Dimens. Syst. Nanostruct.* **2017**, *90*, 204-213.
23. Gang, L.; Guo, S.; Wu, Q.; Wu, L. *Mol. Phys.* **2020**, *118*, e1788190.
24. Delgadillo Armendariz, N. L.; Rangel Vásquez, N. A.; Marquez Brazón, E. A. *Rev. Colomb. Quim.* **2020**, *49*, 12-17.
25. Fakhari, S.; Nouri, A.; Jamzad, M.; Arab-Salmanabadi, S.; Falaki, F. *J. Chin. Chem. Soc.* **2021**, *68*, 67-75.
26. Arshad, M.; Arshad, S.; Majeed, M. K.; Frueh, J.; Chang, C.; Bilal, I.; Niaz, S. I.; Khan, M. S.; Tariq, M. A.; Yasir Mehboob, M. *ACS Omega.* **2023**, *8*, 11318-11325.
27. Perdew, J. P.; Burke, K.; Ernzerhof, M. *Phys. Rev. Lett.* **1996**, *77*, 3865-3868.
28. Krishnan, R.; Binkley, J. S.; Seeger, R.; Pople, J. A. *J. Phys. Chem.* **1980**, *72*, 650-654.
29. Stefan, G.; Jens, A.; Stephan, E.; Helge, K. *J. Chem. Phys.* **2010**, *132*, 154104.
30. Glendening, E. D.; Landis, C. R.; Weinhold, F. *J. Comput. Chem.* **2013**, *34*, 1429- 1437.
31. Perdew, J. P.; Burke, K.; Ernzerhof, M. *Phys. Rev. Lett.* **1997**, *77*, 3865-3868.
32. Pritchard, B. P.; Altarawy, D.; Didier, B.; Gibson, T. D.; Windus, T. L. *J. Chem. Inf. Model.* **2019**, *59*, 4814-4820.
33. Parr, R. G.; Pearson, R. G. *J. Am. Chem. Soc.* **1983**, *105*, 7512-7516.
34. Parr, R. G.; Donnelly, R. A.; Levy, M.; Palke, W. E. *J. Chem. Phys.* **1978**, *68*, 3801- 3807.

J. Mex. Chem. Soc. **2025**, *69*(3)
Regular Issue
©2025, Sociedad Química de México
ISSN-e 2594-0317

35. Parr, R. G.; Szentpály, L. V.; Liu, S. *J. Am. Chem. Soc.* **1999**, *121*, 1922-1924.
36. Janaki, C. S.; Sailatha, E.; Gunasekaran, S.; Kumaar, G. R. *Int. J. TechnoChem. Res*. **2016**, 91-104.
37. Jeffrey, G.A., in: *An introduction to hydrogen bonding*, Oxford University Press: New York and Oxford., **1997**.
38. Cordero, B.; Gómez, V.; Platero-Prats, A. E.; Revés, M.; Echeverría, J.; Cremades, E.; Barragán, F.; Alvarez, S. *Dalton Trans.* **2008**, 2832-2838.
39. Dannenberg, J. J. *J. Am. Chem. Soc.* **1998**, *120*, 5604-5604.
40. Yu, J.; Su, N. Q.; Yang, W. *JACS Au*. **2022**, *2*, 1383-1394.
41. Weinhold, F.; Landis, C. R., in: *Valency and bonding: a natural bond orbital donor- acceptor perspective*, Cambridge University Press, Cambridge, **2005**.
42. Hernández, B.; Pflüger, F.; Kruglik, S. G.; Cohen, R; Ghomi, M.; *J. Pharm. Biomed. Anal.* **2015**, *114*, 42-48.
43. Mondal, S.; Samajdar, R. N.; Mukherjee, S.; Bhattacharyya, A. J.; Bagchi, B. *J. Phys. Chem. B* **2018**, *122*, 2227-2242.